Deep Learning-based Fingerprinting for Outdoor UE Positioning Utilising Spatially Correlated RSSs of 5G Networks

Al-Tahmeesschi, Ahmed

IEEE
2022

Al-Tahmeesschi , A , Talvitie , J , Lopez-Benitez , M & Ruotsalainen , L 2022 , Deep Learning-based Fingerprinting for Outdoor UE Positioning Utilising Spatially Correlated RSSs of 5G Networks . in J Nurmi , ES Lohan , JT Sospedra , H Kuusniemi & A Ometov (eds) , 2022 INTERNATIONAL CONFERENCE ON LOCALIZATION AND GNSS (ICL-GNSS) . International Conference on Localization and GNSS , IEEE , 12th International Conference on Localization, Navigation and GNSS (ICL-GNSS) , Tampere , Finland , 07/06/2022 . https://doi.org/10.1109/ICL-GNSS54081.2022.9797017

http://hdl.handle.net/10138/350530
https://doi.org/10.1109/ICL-GNSS54081.2022.9797017

acceptedVersion

Deep Learning-based Fingerprinting for Outdoor UE Positioning Utilising Spatially Correlated RSSs of 5G Networks

Ahmed Al-Tahmeesschi[1], Jukka Talvitie[2], Miguel López-Benítez[3,4], and Laura Ruotsalainen[1]

[1]Dept. of Computer Science, University of Helsinki, Helsinki, Finland
[2]Unit of Electrical Engineering, Tampere University, Tampere, Finland
[3]Dept. of Electrical Engineering and Electronics, University of Liverpool, United Kingdom
[4]ARIES Research Centre, Antonio de Nebrija University, Spain

***Abstract*—Outdoor user equipment (UE) localisation has attracted a significant amount of attention due to its importance in many location-based services. Typically, in rural and open areas, global navigation satellite systems (GNSS) can provide an accurate and reliable localisation performance. However, in urban areas GNSS localisation accuracy is significantly reduced due to shadowing, scattering and signal blockages. In this work, the UE positioning assisted by deep learning in 5G and beyond networks is investigated in an urban area environment. We study the impact of utilising the spatial correlation in the received signal strengths (RSSs) on the UE positioning accuracy and how to utilise such correlation with deep learning algorithms to improve the localisation accuracy. Numerical results showed the importance of utilising the spatial correlation in the RSS to improve the prediction accuracy for all of the considered models. In addition, the impact of varying the number of access points (APs) transmitters on the localisation accuracy is also investigated. Numerical results showed that a lower number of APs may be sufficient when not considering uncertainties in RSS measurements. Moreover, we study how much the degrading effect of RSS uncertainty can be compensated for by increasing the number of APs.**

Keywords*— *5G, beamforming, deep learning, fingerprinting, UE positioning.

I. Introduction

Outdoor localisation has been an active field of research in recent years with accuracy and robustness being key enablers for several emergency and commercial location-based services [1]. In United States, the Federal Communications Commission (FCC) has set the requirements for positioning error to be a maximum of 50m for horizontal error and less than 5m for vertical error for emergency calls [2]. Moreover, the 3rd Generation Partnership Project (3GPP) has set even tighter accuracy values depending on the application. For instance, the positioning requirements for emergency calls are in tens of meters, while the requirement decreases to a few decimeters within indoor factories and one decimeter for vehicle-to-everything (V2X) in autonomous driving vehicles [3]. While global navigation satellite systems (GNSS) are capable of providing both meter level accuracy in open and rural areas, the GNSS positioning accuracy degrades significantly in urban and densely built-up areas due to various reasons including blockage, scattering and multipath propagation [4]. This work considers the positioning of UEs operating in an urban area scenario.

It is envisioned that in 5G and beyond 5G (B5G) networks the user equipment (UE) will be capable of running machine learning algorithms. In addition, 5G networks have already adapted millimetre wave (mmWave) along with massive multiple-input-multiple-output (MIMO) technologies to provide extremely high data rates to users. But using high-frequency bands has its own drawbacks including a severely high pathloss. In order to compensate for such losses, beamforming techniques are used to direct the transmission by providing a large directional gain [5]. Additionally, the spatial distance between the mmWave transmitters is reduced to the order of a hundred meters. Thus, it is desired to be able to perform localisation at both network and UE ends. Several works in the literature have considered cellular-based localisation systems for both indoor and outdoor scenarios [6]. Typical and low complexity approaches such as the K nearest neighbour (KNN) machine learning approach does not provide sufficient UE location accuracy due to the large fluctuations in the received signal strength [7].

Deep learning approaches have been utilised recently for both indoor and outdoor fingerprinting [8–14]. In [8] the authors demonstrated the correlation in the received signal strengths (RSS) in time and their impact on improving the localisation accuracy. Our work is different in the sense that we benefit from the spatial correlation of different RSSs and their impact to improve the localisation accuracy. The authors in [10] used the RSSs from multiple beams as input to the fingerprinting multilayer perceptron (MLP). In [11] and [12], the authors extracted features from the signal and beams such as angle of beam departure, cell identity and channel bandwidth and combined them using an MLP.

While the mentioned works have utilised deep learning for fingerprinting, they do not provide a comprehensive understanding for the outdoor urban radio environment and how the RSSs are correlated among locations at relatively close proximity (in meters). In this work, we aim to exploit such spatial

978-1-6654-0575-1/22/$31.00

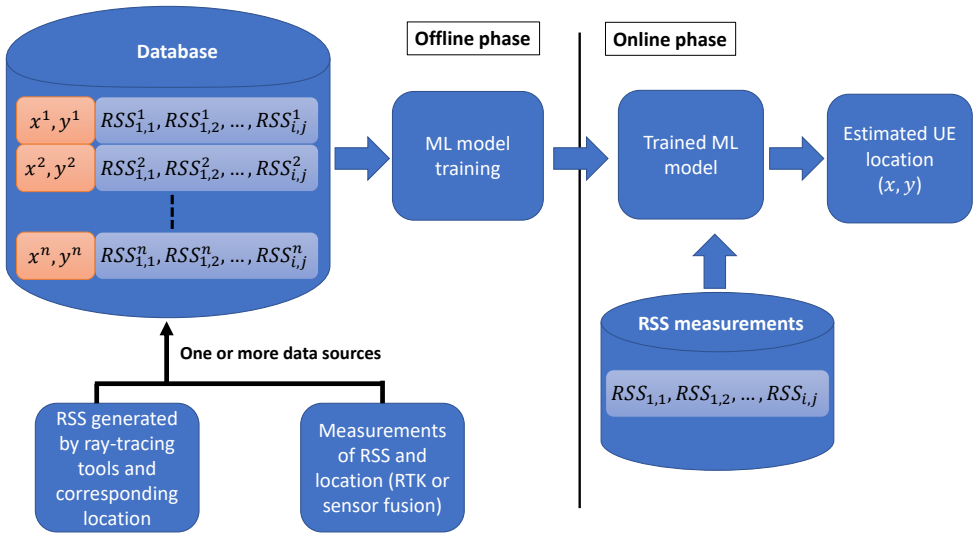

Fig. 1. Schematic diagram of the offline and online phases for machine learning (ML) fingerprinting process. $RSS^n_{i,j}$ is the received signal strength from the i_{th} BS, j_{th} beam at the n_{th} location.

correlation in the RSSs to improve the localisation accuracy using a deep learning approach. Another open question we aim to answer is how many access points (APs) representing base stations (BSs) are required in order to achieve sub-meter level localisation accuracy. Lastly, this work considers the horizontal localisation accuracy (in terms of x and y coordinates) thus the horizontal term will be omitted during the discussion in the rest of the work.

The contributions of this work are outlined as follows:

1) Investigated the performance of multiple deep learning algorithms to estimate the fingerprinting accuracy on a dataset generated by a specialised ray-tracing simulation approach in a built-up city scenario and the algorithms capability to learn from the available spatial correlation in RSS.
2) Analysed different AP deployment strategies in the considered area by evaluating the positioning errors in terms of the number of APs used for UE positioning.
3) Demonstrated the importance of increasing the number of considered APs for localisation and their capability to reduce the uncertainties in RSS measurements.

The remainder of this paper is organised as follows. First, Section II discusses the RSS-based fingerprinting approach. Section III presents the system setup for the conducted experiments. Section IV presents the considered machine and deep learning models for UE localisation. The performance of the considered models is evaluated and discussed in Section V. Finally, Section VI summarises and concludes this work.

II. RSS-based Fingerprint positioning

The fingerprinting localisation includes two phases, the offline and online phase as shown in Fig. 1. During the offline phase, mmWave RSSs are either measured or generated using a ray-tracing tool at several known locations. For the case of a real-life measurements scenario, either a Real-Time Kinematic (RTK) positioning [15] or a sensor fusion approach [16] can be used to accurately extract the RSS measurements' locations (ground truth labels). The RSS values are labelled with their locations to form the database (also referred to as radio environment map [17]). The collected database is used to train the fingerprinting model. During the online phase, all the collected RSS values for the unknown location are compared with the radio environment map to retrieve the measurement location. This work considers a deep learning regression approach to infer the UE coordinates (in terms of x and y) which corresponds to the given RSS values as can be seen in Fig. 1.

III. Simulation environment

In this section, the system setup considered in this work is described. In order to generate a realistic simulation environment, the 5G mmWave signals are generated using a ray-tracing-based approach, as recommended by 3GPP [18], and for the city layout, the Madrid grid is selected as recommended by the METIS project in [19]. Furthermore, the ray-tracing-based channel measurements are obtained by Wireless InSite software [20]. A similar simulation environment setup can also be found in [21]. For our research, a specific segment of the Madrid grid is selected with 7 APs operating at 28GHz. The AP height is set to 9m and each AP includes two sectors. Each sector includes a patch antenna element arranged in a uniform linear array. The transmitted power per sector is set to 30dBm.

During the simulation, a single UE moves along the blue line (as can be seen in Fig. 2). The measurement resolution is 1m which gave us a total of 1118 unique locations. In total, 250432 measurements were recorded where each measurement corresponds to the RSS from a specific beam and a measurement location (i.e., x, y coordinates). The simulated RSS observed at each UE location is based on the beam RSS. In practice, the RSS measurements obtained by the UE

TABLE I
SIMULATION PARAMETER

Parameter	Value
Number of sites	7
Number of sectors per site	2
Number of beams per sector	16
AP height	9m
Carrier frequency	28GHz
Resolution of data points	1m
AP Tx Power per sector	30dBm

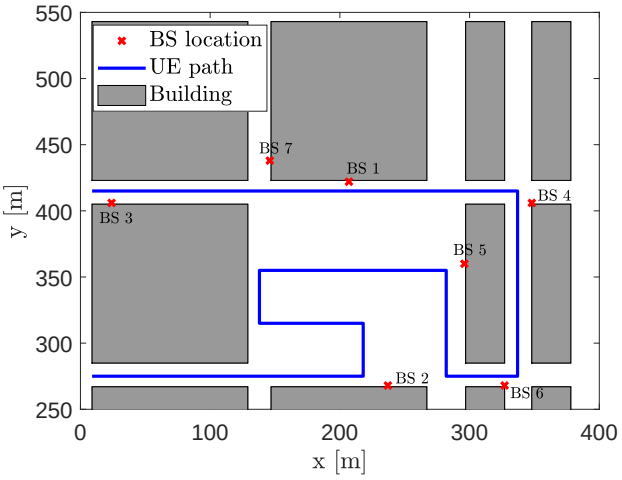

Fig. 2. Urban area network visualisation with 7 beamforming capable BSs. A user is navigating in the environment and measuring RSS.

are based on 3GPP-specified synchronization signal blocks (SSBs) transmitted by each BS over 32 beams [22]. The utilised beamforming is implemented following the phased-array principle. Each of the two sectors found in a single BS is designated to cover 90 degrees and the 16 beams set for each sector are uniformly spaced (i.e., each AP covers 180 degrees). The detailed simulation parameters used for the simulation are provided in Table I and Fig. 2 shows the considered Madrid grid segment along with the user path and BS locations in the map. Furthermore, in order to evaluate the system's ability to suppress uncertainty in RSS measurements due to various reasons such as noise, interference and human body blockages, we follow a similar approach to [21] and additionally add uncertainties to the RSS measurements generated following a Normal distribution $\mathcal{N}(\mu, \sigma^2)$ with mean $\mu_n = 0$ and standard deviation $\sigma_n \in \{0, 1, 2, 3\}$ in dB. Thus, we have 4 datasets in total with different uncertainty levels in RSS.

IV. Machine and Deep Learning Techniques

This section discusses the considered machine and deep learning models for the UE positioning.

A. KNN model

For baseline machine learning fingerprinting approach, the K-nearest neighbour algorithm is considered as it is one of the most popular algorithms for RSS-based fingerprinting [23]. In a traditional KNN, the position of the UE is estimated based on the mean of K number of the nearest neighbours locations. The Euclidean distance is used to find the nearest neighbours from the accumulated database.

B. MLP

An MLP is a feed-forward type neural network based on the backpropagation algorithm [24]. The considered MLP model is a sequential one with three hidden layers, which takes RSS measurements as input and returns the inferred location as output. The considered MLP's architecture for the RSS fingerprinting is given as follows:

- Input layer with Z×I×J RSS measurements vector, where I is the number of APs (from 2 to 7), J=32 is the number of beams and Z is the number of look-backs (from 1 to 40).
- Densely connected layer with 1024 neurons and a Rectified Linear Unit (ReLU) activation function.
- Densely connected layer with 512 neurons and a ReLU activation function.
- Densely connected layer with 64 neurons and a ReLU activation function.
- Densely connected output layer with 2 neurons and a linear activation function for the UE positioning estimation.

The activation function is used to describe the non-linear properties between neuron input and output. For MLP, a ReLU activation function which is defined as positive part of it is argument and given as $\psi(p) = max(0, p)$ [25]. We define the look-back as how many previous RSSs (i.e., RSSs from the previous locations) are used in order to predict the current location. The model is trained with a mean squared error (MSE) loss function which represents the error of the Euclidean distance between the UE true and estimated locations. In addition to the proposed model, other MLP models such as the ones considered in [14] and [13] were also tested, but we found out that the proposed model provided a slightly higher UE position estimation accuracy.

C. LSTM and GRU models

The long short-term memory (LSTM) network is a variation of recurrent neural networks (RNNs) which is typically used for time series data types. It was first proposed in [26] as an improvement over RNN to solve long-term dependency. For this work, several architectures have been tested, such as increasing the number of hidden layers and it was found that three hidden layers gave the highest localisation accuracy. The considered LSTM architecture for the RSS fingerprinting is given as follows:

- Input layer with (Z, I×J) RSS measurements array, where I is the number of APs (from 2 to 7), J=32 is the number of beams and Z is the number of look-backs (from 1 to 40).
- An LSTM layer with 1024 neurons and a hyperbolic tangent (Tanh) activation function.
- An LSTM layer with 512 neurons and a hyperbolic tangent (Tanh) activation function.

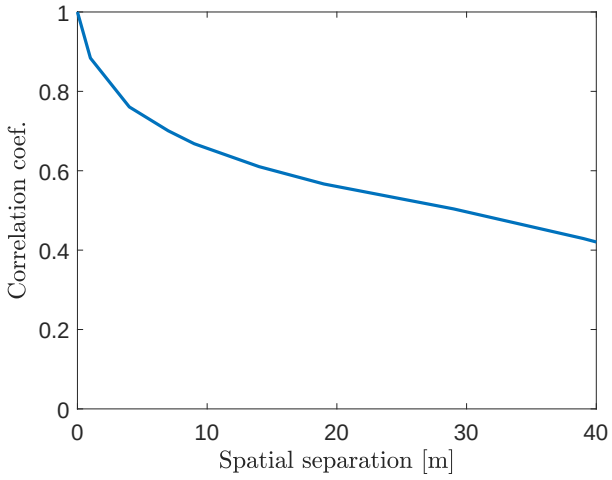

Fig. 3. The correlation coefficient as a function of distance for AP1. The x axis represents the separation between RSSs.

- An LSTM layer with 64 neurons and a hyperbolic tangent (Tanh) activation function.
- Densely connected output layer with 2 neurons and a linear activation function for the UE positioning estimation.

The LSTM model is also trained with a mean squared error (MSE) loss function.

Another RNN variant is the gated recurrent unit (GRU) [27]. The GRU generally has a comparable performance to LSTM but it is computationally more efficient (has a less complex structure). The same model is considered for both LSTM and GRU as the two models are associated with time series datasets and we wanted to compare their accuracy.

V. Experimental evaluation

In this section, the positioning accuracies of the considered models are presented. For this work, two metrics, namely the mean ($\bar{E}$) and variance (σ^2), of the Euclidean distance between the estimated UE position and the actual position are considered and they are defined as,

$$\bar{E} = \frac{1}{N}\sum_{n=1}^{N} x_n, \tag{1}$$

$$\sigma^2 = \frac{1}{N}\sum_{n=1}^{N} (x_n - \bar{E})^2, \tag{2}$$

where, x_n is the Euclidean distance between estimated and actual UE position for the n^{th} sample.

In this work, Python 3 language is used alongside TensorFlow [28] as backend. Adam optimiser [29] was used as it is by far the most commonly utilised optimiser in the current deep learning domain [30]. The dataset is split into training, validation and testing subsets with 55-20-25 ratios with shuffling. In addition, k-fold validation was also used which yields in different training, validation and testing sub-datasets at each training. Given that neural networks models are stochastic, hence, different weights will result at each training time even when the same model configuration is utilised. In order to address the model accuracy evaluation, each model configuration is evaluated multiple times (20 times in our case). The reported positioning accuracy is averaged across all of the evaluations. The training batch size is set to 64 and the learning rate is set to 0.001. All simulations were conducted with a maximum number of epochs set to 4000. An early stopping algorithm is utilised to prevent overfitting (during training stage) with an early stop value of 300 iterations [31]. A separate MinMax scaler was applied for the RSS dataset and the UE coordinates as there is a significant difference between their values (the RSS dataset is between -19 and -100 dBm, while the UE coordinates are between 0 and 550 meters) [32].

TABLE II
KNN UE location estimation accuracy (horizontal accuracy) for different K values, look-back = 1 and all 7APs.

K nearest neighbour Look-back = 1	Mean $\bar{E}$ (m)	Variance σ^2 $(m)^2$
1	3.442	0.037
2	3.304	0.036
3	3.851	0.031
4	4.389	0.035
5	4.924	0.036
6	5.422	0.058

First, the spatial correlation in the RSSs is discussed, which is a feature exploited in this work. For instance, the averaged spatial Pearson's correlation coefficient of the RSSs (across all 32 beams) from AP1 is shown in Fig. 3. As it can be appreciated, the smaller the spatial separation between RSSs is the higher the correlation coefficient value.

Next, the configuration of KNN is discussed. Given that the number of K neighbours depends on the radio environment and the UE path. Hence, several K values are investigated to find the highest positioning accuracy. Table II, shows the positioning accuracy of different K values for the considered scenario. These results are obtained from a single look-back (i.e., only the current RSSs are considered) and when all the 7APs are present under zero level uncertainty (i.e., $\sigma_n = 0$ dB). As it can be concluded, $K = 2$ provides the highest location accuracy with an average positioning accuracy of 3.304 m. Higher K vales ($K > 6$) were also investigated, but we only found them to reduce the positioning accuracy. Thus, we decided not to include them in the results.

Next, Table III shows the localisation accuracy of different deep learning (DL) algorithms (i.e., MLP, LSTM and GRU) and machine learning (ML) algorithm (i.e., KNN) when all of the seven APs are used for UE localisation. Moreover, the capability of these models to learn from the spatial correlations of the RSS dataset are investigated too. In other words, the effect of different number of RSS historical values (i.e., look-backs) are investigated to demonstrate the importance of adding more look-backs under a baseline scenario (i.e., under no uncertainties $\sigma_n = 0$ dB). The first observation is that all models benefit from adding more look-backs and experience a performance improvement with a larger number

of look-backs. It is worth noting that such improvement did not continue with larger look-backs and it saturates around some look-backs value. For instance, the considered LSTM saturates at 20 look-backs, while the GRU saturates at 30 look-backs. In addition, both KNN and MLP have relatively similar positioning accuracies but are worse than the other considered algorithms (i.e., GRU and LSTM) in terms of both the average $\bar{E}$ and the variance σ^2. The LSTM and GRU models have relatively similar positioning accuracies with an advantage for the LSTM. For instance, at 20 look-backs, the LSTM provided an average error and variance of 0.523m and 0.009m^2 respectively, while the GRU provided an average error 0.655m and variance of 0.011m^2. Thus, it can be concluded that LSTM is a better model to capture the spatial correlations in the RSS dataset and is a better option for fingerprinting.

The cumulative distribution function (CDF) for the positioning error of the considered models (at their best look-back value) are shown in Fig. 4. The results are consistent with the ones obtained in Table III with having the LSTM giving the best performance among the considered models in this work. In addition, both the KNN and MLP have similar performances. The stairs shape of the KNN's CDF is due to the fact that KNN is a clustering algorithm and therefore it has a finite precision as a result of its discrete output.

Since LSTM provided the highest average localisation accuracy among the tested models, next we study the effect of changing the number of serving APs with LSTM and their impact on positioning accuracy as can be seen in Table IV. As it can be appreciated, having a larger number of APs generally improves the UE location estimation accuracy and reduces the variance of estimations. For instance, to ensure sub-meter accuracy, having at least 3 APs with 10 look-backs is essential. As for higher accuracies such as an average of around a half meter, then the number of APs should be increased to a minimum of 5 APs and with a relatively high number of look-backs, in our simulation 20 look-backs were required to reach such high accuracy as it can be concluded from Table IV.

Fig. 5 shows the empirical CDF of localisation error of multiple APs combinations and different look-backs. As it can be appreciated, 5 APs have similar localisation accuracy compared to 7 APs at 20 look-backs.

The results obtained from Table IV and Fig. 5 imply the possibility of obtaining a high level of accuracy while using less number of APs by increasing the number of look-backs. In practice, maintaining a large number of APs is not guaranteed and it can be compensated by increasing the number of look-backs which only requires slightly increasing the UE or operator memory space to store RSS values.

Finally, we analyse the capability of the LSTM model to mitigate different uncertainty values in the measurements. As can be inferred from Table V, having a small uncertainty value (i.e., σ_n = 1 dB) does not impact the prediction accuracy and an average of around 1 m accuracy could be attained for both 5 APs and 7 APs. For the case of high RSS uncertainty (i.e., σ_n = 3 dB), having 7 APs can improve the localisation accuracy by 1 meter over only having 5 APs. From these results, it can be concluded that APs diversity improves the LSTM capability

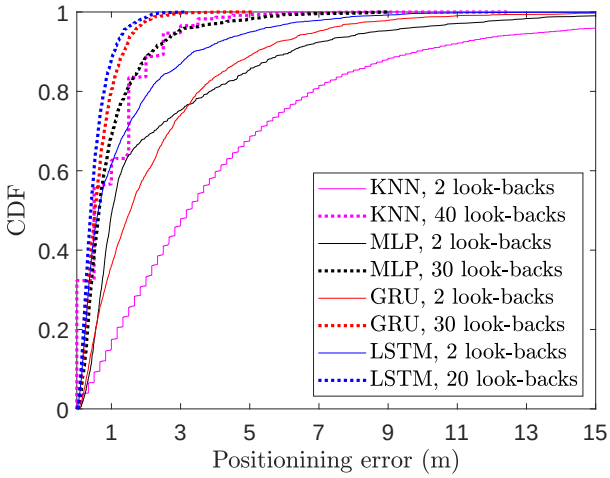

Fig. 4. Empirical CDF of the UE horizontal positioning estimation error of RSS fingerprinting for 7 APs.

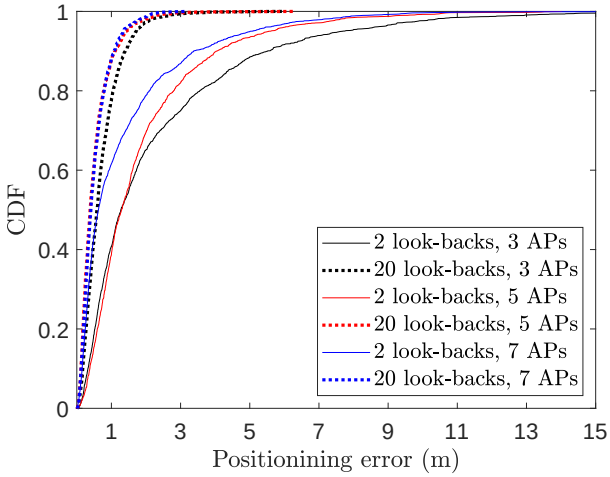

Fig. 5. Empirical CDF of the UE horizontal positioning estimation error of RSS fingerprinting versus the number of APs.

to deal with RSS uncertainty and increasing the number of APs can overcome the degrading impact of RSS uncertainty on the UE localisation.

Fig. 6 shows the CDF of positioning accuracy of different RSS uncertainty levels for 5 APs and 7 APs. As it can be appreciated, 5 APs have similar localisation accuracy compared to 7 APs at σ_n = 0 dB. However, once the uncertainties are included, 7 APs positioning accuracy surpasses 5 APs with a significant margin. Thus it can be concluded that having more number of APs is essential to alleviate the uncertainties in RSS.

VI. Conclusions

This work has demonstrated that the spatial correlation in the RSS is an essential feature and having it alone is sufficient to achieve sub-meter level positioning accuracy without the requirement to modify current standards nor applying fusion methods.

TABLE III
POSITIONING HORIZONTAL ACCURACY FOR THE CONSIDERED MACHINE AND DEEP LEARNING ALGORITHMS.

Look-back	KNN		MLP		GRU		LSTM	
	$\bar{E}$	σ^2	$\bar{E}$	σ^2	$\bar{E}$	σ^2	$\bar{E}$	σ^2
1	3.304	0.036	2.663	0.785	2.202	0.927	1.929	0.450
2	2.565	0.028	2.367	0.278	2.286	0.512	1.351	0.223
5	1.755	0.011	1.949	0.441	1.457	0.116	1.067	0.326
8	1.412	0.014	1.529	0.332	1.181	0.025	0.774	0.040
10	1.271	0.006	1.440	0.234	1.256	0.028	0.697	0.018
15	1.125	0.007	1.395	0.190	1.170	0.074	0.647	0.007
20	1.065	0.005	1.235	0.332	0.877	0.017	0.523	0.009
30	0.986	0.004	0.998	0.063	0.655	0.011	0.535	0.010
40	0.984	0.003	1.247	0.058	0.809	0.008	0.551	0.080

TABLE IV
POSITIONING HORIZONTAL ACCURACY WITH LSTM AND VARYING NUMBER OF APS.

Look-back	2APs		3APs		4APs		5APs		6APs		7APs	
	$\bar{E}$	σ^2	$\bar{E}$	σ^2	$\bar{E}$	σ^2	$\bar{E}$	σ^2	$\bar{E}$	σ^2	$\bar{E}$	σ^2
1	3.333	1.163	3.435	1.064	2.284	0.631	1.809	0.560	2.098	0.759	1.929	0.450
2	2.994	0.948	2.300	0.521	1.875	0.430	1.874	0.454	1.900	0.400	1.351	0.223
5	2.377	0.723	1.546	0.034	1.435	0.041	1.158	0.033	1.060	0.041	1.067	0.326
8	1.955	0.123	1.068	0.116	1.328	0.058	0.995	0.011	0.930	0.080	0.774	0.040
10	1.802	0.023	0.991	0.002	0.839	0.051	0.748	0.060	0.738	0.069	0.697	0.018
15	1.600	0.048	0.697	0.011	0.633	0.021	0.582	0.014	0.764	0.074	0.647	0.007
20	1.402	0.057	0.707	0.081	0.618	0.051	0.527	0.007	0.534	0.011	0.523	0.009

TABLE V
HORIZONTAL POSITIONING ACCURACY FOR LSTM (7APS) VERSUS DIFFERENT UNCERTAINTY-LEVELS IN RSS

Uncertainty level σ_n in dB	5 APs		7 APs	
	$\bar{E}$	σ^2	$\bar{E}$	σ^2
0	0.527	0.007	0.523	0.009
1	1.120	0.211	0.988	0.054
2	1.605	0.889	1.126	0.245
3	3.291	3.553	2.120	2.211

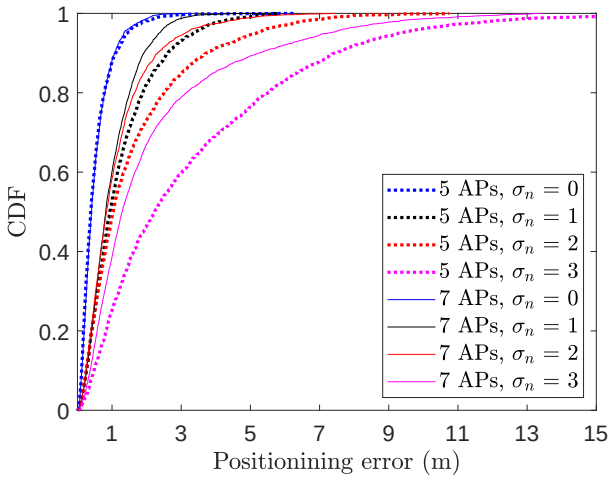

Fig. 6. Empirical CDF of the UE horizontal positioning estimation error under RSS uncertainties for 5 APs and 7 APs.

This work studied the accuracy of UE positioning in an urban environment. The performance of state of the art approaches is explored for outdoor positioning including machine and deep learning algorithms with a large emphasis on the capability of the considered models to learn from the spatial correlation in the RSS dataset. The obtained numerical results showed that deep learning approaches, specifically the LSTM, provided the best capability in providing accurate UE localisation with an average of around a half meter positioning accuracy based on the RSS only. This result demonstrates the importance of RSS spatial correlations in improving the localisation accuracy even when the considered ray-tracing dataset has a one meter UE separation. In addition, the effect of varying the number of APs used for localisation has been investigated.

The obtained numerical results demonstrated the importance of utilising the spatial correlation in the RSS on improving UE localisation accuracy. In addition, a lower number of APs can be sufficient to have high localisation accuracy under no RSS measurement uncertainties. While, the degrading effect of RSS uncertainty can be mitigated by increasing the number of APs (e.g., up to 1 meter accuracy improvement when increasing from 5 to 7 APs).

ACKNOWLEDGEMENT

This work was supported by the Academy of Finland Flagship programme: Finnish Center for Artificial Intelligence FCAI, Department of Computer Science, University of Helsinki.

REFERENCES

[1] Q. D. Vo and P. De, "A survey of fingerprint-based outdoor localization," *IEEE Communications Surveys Tutorials*, vol. 18, no. 1, pp. 491–506, 2016.

[2] FCC, *PS docket No 07-114*. Wireless E911 location accuracy requirements, Jan. 2015.

[3] 3GPP, *Service requirements for the 5G system*. 3rd Generation Partnership Project (3GPP), Technical Specifications (TS) 22.261, 12, version 18.1.0., 2016.

[4] T. Kos, I. Markezic, and J. Pokrajcic, "Effects of multipath reception on GPS positioning performance," in *Proceedings ELMAR-2010*, 2010, pp. 399–402.

[5] S. Hur, T. Kim, D. J. Love, J. V. Krogmeier, T. A. Thomas, and A. Ghosh, "Millimeter wave beamforming for wireless backhaul and access in small cell networks," *IEEE Transactions on Communications*, vol. 61, no. 10, pp. 4391–4403, 2013.

[6] J. A. del Peral-Rosado, R. Raulefs, J. A. LÃşpez-Salcedo, and G. Seco-Granados, "Survey of cellular mobile radio localization methods: From 1G to 5G," *IEEE Communications Surveys Tutorials*, vol. 20, no. 2, pp. 1124–1148, 2018.

[7] S. H. Javadi, H. Moosaei, and D. Ciuonzo, "Learning wireless sensor networks for source localization," *Sensors*, vol. 19, no. 3, 2019. [Online]. Available: https://www.mdpi.com/1424-8220/19/3/635

[8] B. Xu, X. Zhu, and H. Zhu, "An efficient indoor localization method based on the long short-term memory recurrent neuron network," *IEEE Access*, vol. 7, pp. 123 912–123 921, 2019.

[9] J. Gante, L. Sousa, and G. Falcao, "Dethroning GPS: Low-power accurate 5G positioning systems using machine learning," *IEEE Journal on Emerging and Selected Topics in Circuits and Systems*, vol. 10, no. 2, pp. 240–252, 2020.

[10] N. Xu, S. Li, C. S. Charollais, A. Burg, and A. Schumacher, "Machine learning based outdoor localization using the RSSI of multibeam antennas," in *2020 IEEE Workshop on Signal Processing Systems (SiPS)*, 2020, pp. 1–5.

[11] A. Mohamed, M. Tharwat, M. Magdy, T. Abubakr, O. Nasr, and M. Youssef, "Deepfeat: Robust large-scale multi-features outdoor localization in LTE networks using deep learning," *IEEE Access*, vol. 10, pp. 3400–3414, 2022.

[12] M. M. Butt, A. Pantelidou, and I. Z. KovÃącs, "ML-assisted UE positioning: Performance analysis and 5G architecture enhancements," *IEEE Open Journal of Vehicular Technology*, vol. 2, pp. 377–388, 2021.

[13] M. M. Butt, A. Rao, and D. Yoon, "RF fingerprinting and deep learning assisted UE positioning in 5G," in *2020 IEEE 91st Vehicular Technology Conference (VTC2020-Spring)*, 2020, pp. 1–7.

[14] R. Klus, J. Talvitie, and M. Valkama, "Neural network fingerprinting and GNSS data fusion for improved localization in 5G," in *2021 International Conference on Localization and GNSS (ICL-GNSS)*, 2021, pp. 1–6.

[15] P. Reisdorf, T. Pfeifer, J. Breßler, S. Bauer, P. Weissig, S. Lange, G. Wanielik, and P. Protzel, "The problem of comparable gnss results - an approach for a uniform dataset with low-cost and reference data," in *5th Int. Conf. Advances in Vehicular Systems Technologies and Applications*, Nov. 2016.

[16] Q. Li, J. P. Queralta, T. N. Gia, Z. Zou, and T. Westerlund, "Multi-sensor fusion for navigation and mapping in autonomous vehicles: Accurate localization in urban environments," *Unmanned Systems*, vol. 08, no. 03, pp. 229–237, 2020. [Online]. Available: https://doi.org/10.1142/S2301385020500168

[17] K. Sato and T. Fujii, "Kriging-based interference power constraint: Integrated design of the radio environment map and transmission power," *IEEE Transactions on Cognitive Communications and Networking*, vol. 3, no. 1, pp. 13–25, 2017.

[18] 3GPP, "Study on channel model for frequencies from 0.5 to 100 GHz," 3rd Generation Partnership Project (3GPP), Technical Specification (TS) TS 38.901, 01 2020, version 16.1.0. [Online]. Available: https://portal.3gpp.org/desktopmodules/Specifications/SpecificationDetails.aspx?specificationId=3173

[19] V. Nurmela *et al.*, "Deliverable D1.4: METIS channel models." Proc. Mobile Wireless Commun. Enablers Twenty-Twenty Inf. Soc. (METIS), 2015, p. 1.

[20] Remcom. Wireless InSite - 3D wireless prediction software. Accessed: Jan 27, 2021). [Online]. Available: https://www.remcom.com/wireless-insite-em-propagation-software

[21] R. Klus, L. Klus, D. Solomitckii, J. Talvitie, and M. Valkama, "Deep learning-based cell-level and beam-level mobility management system," *Sensors*, vol. 20, no. 24, 2020. [Online]. Available: https://www.mdpi.com/1424-8220/20/24/7124

[22] 3GPP, "NR; Physical layer measurements," 3rd Generation Partnership Project (3GPP), Technical Specification (TS) 38.215, 07 2020, version 15.7.0. [Online]. Available: https://portal.3gpp.org/desktopmodules/Specifications/SpecificationDetails.aspx?specificationId=3217

[23] M. Y. Umair, K. V. Ramana, and Y. Dongkai, "An enhanced K-Nearest Neighbor algorithm for indoor positioning systems in a WLAN," in *2014 IEEE Computers, Communications and IT Applications Conference*, 2014, pp. 19–23.

[24] J. Schmidhuber, "Deep learning in neural networks: An overview," *Neural Networks*, vol. 61, pp. 85 – 117, 2015.

[25] X. Glorot, A. Bordes, and Y. Bengio, "Deep sparse rectifier neural networks," in *Proceedings International Conference on Artificial Intelligence and Statistics*, 2011, pp. 315–323.

[26] S. Hochreiter and J. Schmidhuber, "Long short-term memory," *Neural computation*, vol. 9, pp. 1735–80, 12 1997.

[27] J. Chung, C. Gulcehre, K. Cho, and Y. Bengio, "Empirical evaluation of gated recurrent neural networks on sequence modeling," *arXiv:1412.3555*, 2014.

[28] M. Abadi, A. Agarwal, P. Barham, E. Brevdo, Z. Chen, C. Citro, and et al., "TensorFlow: Large-scale machine learning on heterogeneous systems," 2015, software available from tensorflow.org.

[29] D. P. Kingma and J. Ba, "Adam: A method for stochastic optimization," in *International Conference on Learning Representations (ICLR)*, 2015.

[30] C. Zhang, P. Patras, and H. Haddadi, "Deep learning in mobile and wireless networking: A survey," *IEEE Communications Surveys Tutorials*, vol. 21, no. 3, pp. 2224–2287, 2019.

[31] L. Prechelt, *Early Stopping — But When?* Berlin, Heidelberg: Springer Berlin Heidelberg, 2012, pp. 53–67. [Online]. Available: https://doi.org/10.1007/978-3-642-35289-8_5

[32] F. Pedregosa, G. Varoquaux, A. Gramfort, V. Michel, B. Thirion, O. Grisel, M. Blondel, P. Prettenhofer, R. Weiss, V. Dubourg, J. Vanderplas, A. Passos, D. Cournapeau, M. Brucher, M. Perrot, and E. Duchesnay, "Scikit-learn: Machine learning in Python," *Journal of Machine Learning Research*, vol. 12, pp. 2825–2830, 2011.